Acoustic-optical Image Denoising Using Alpha-Stable Multivariate Shrinkage Function in the Contourlet Domain

[1,2*]Huimin Lu, [1*]Seiichi Serikawa, [1]Lifeng Zhang and [3*]Shota Nakashima

Abstract

We describe a method for removing acoustic-optical image noise, based on a statistical model of the decomposed contourlet coefficients. This method proposes an alpha-stable multivariate shrinkage (MS) probability density function to model neighborhood contourlet coefficients. Then, according to the proposed PDF model, we design a maximum a posteriori (MAP) estimator, which relies on a Bayesian statistics representation for the contourlet coefficients of acoustic-optical images. There are two obvious virtues of this method. Firstly, contourlet transform decomposition is prior to curvelettransform by using ellipse sampling grid. Secondly, non-Gaussian multivariate shrinkage model is more effective in presentation of the acoustic-optical image contourlet coefficients. Some comparisons with the best available results will be presented in order to illustrate the effectiveness of the proposed method.

Keywords: α -stable Distribution, contourlet transform, image denoising, statistical modeling, deep-sea signal processing

*CorrespondingAuthor: Huimin Lu
(E-mail:rikukeibin@gmail.com).
[1]Kyushu Institute of Technology, Japan
[2]Japan Society for the Promotion of Science, Japan
[3]Yamaguchi University, Japan

1. Introduction

Typically, acoustics and videos are the most suitable ways to create an understanding of the geometry and appearance of the underwater environment [15]. However, in the deep sea, the nature light is not available (the nature light approximately 200 meters below the surface of the ocean). Even if the artificial light is applied on Autonomous Underwater Vehicles (AUV) or Remotely Operated Vehicles (ROV), the visible range is very limited, such as the wavelength of the light is short and the turbid water affection is highly. For these reasons, sonar systems are widely used to obtain acoustic images of the seabed.

Recently, an acoustic-optical camera DIDSON [1] can acquire high-resolution ultrasonic images with imaging device is proposed. Which is useful for offshore guidance, fish monitor, hydrothermal vents and methane hydrate survey. Despite the quality of the video sequences is image likely, it still has shortcomings compared with normal optical cameras. With limitation of sight range, there are low signal-to-noise ratio, and low resolution et. al [16], [17].

To some extent, the above drawbacks can be solved by image denoising. Some research has addressed the development of statistical models of wavelet coefficients of images [2], [3], [4]. However, the major drawback for wavelets in two-dimensions or higher is their limited ability in capturing directional information. To overcome this deficiency, some researchers have recently considered multiscale and directional representations that can well capture the geometrical structures such as wedgelets [5], bandelets [6], curvelets [7], [8] and contourlets [9], [12]. Using curvelet transform for decomposition, blocks must be overlapped together to avoid the boundary effect. Therefore, redundancy is higher in this implementation algorithm. Additionally, the curvelet transform is based on ridgelet transform, which the key step is the Cartesian to polar conversion. It is hard to Cartesian-Polar conversion. Luckily, the contourlet transform is a “true” two-dimensional transform that can capture the intrinsic geometrical structure. Contourlet transform represents better the salient features of the image such as edges, lines, curves, and contours, than wavelet transform because of its anisotropy and directionality.

The organization of this paper is as follows: In Section 2, the contourlet-based alpha-stable multivariate shrinkage (□ MS) method will be discussed. We will demonstrate an image denoising algorithm to exploit interscale dependencies, and also apply the contourlet □ MS model in acoustic-optical image and natural image denoising in Section 3. Finally, a conclusion is presented in Section 4.

2. Proposed Moedl

In this section, we propose a new model for non-Gaussian image denoising, which based on Bayesian MAP estimator rule. “g” is equally spaced in the samples of a real-valued image. n is i.i.d. normal random variables. The image with noise x can be expressed as

$$x = g + n, \quad (1)$$

In the contourlet domain, the problem can be formulated as

$$y = s + n, \quad (2)$$

where y = (y1, y2, ..., yM) is the noise contourlet coefficient, s = (s1, s2, ..., sM) is the true coefficient, and n = (n1, n2, ..., nM) is the independent noise. The standard MAP estimator for Eq.(2) is

$$\hat{s}(y) = \arg\max_s p_{s|y}(s \mid y) \quad (3)$$

Using the Bayes rule, the Eq. (3) is equivalent to

$$\begin{aligned} \hat{s}(y) &= \arg\max_s [p_{y|s}(y \mid s)\, p_s(s)] \\ &= \arg\max_s p_n(y-s)\, p_s(s) \end{aligned} \quad (4)$$

The Eq.(4) is equivalent to

$$\hat{s}(y) = \arg\max_s [\log(p_n(y-s)) + \log(p_s(s))] \quad (5)$$

The spherically-contoured zero-mean *d*-dimensional BKF density is

$$p_s(s) = \frac{2}{(2\pi c)^{d/2}\Gamma(p)} \left(\frac{\sqrt{2c}}{\| s \|}\right)^{d/2-p} K_{1-p}\left(\sqrt{\tfrac{2}{c}}\, \| s \|\right) \quad (6)$$

where, $K_\lambda(u)$ is the modified Bessel function. *c* and *p* are the scale parameter and shape parameter. In this paper, we propose a simple non-Gaussian multivariate pdf to model the noise-free coefficients, considering the relationship among a coefficient, neighbors, cousins and parent.

$$p_Y(y) = \frac{\exp\left(\frac{\sigma_n^2}{c}\right)}{(2\pi c)\Gamma(p)} \times \sum_{j=0}^{\infty}\left(-\frac{\sigma_n^2}{c}\right)\frac{(p-1)_j}{j!}\Gamma\left(p-\frac{d}{2}-j, \frac{\sigma_n^2}{c}; \frac{\|c\|^2}{2c}\right) \quad (7)$$

with$j$ factor in both the numerator and denominator of the fraction. "σn" is the standard deviation of the noise coefficients. In Ref. (9), the variables y=*sqrt*(|| y_i ||^2+|| $y_i^{[p]}$ ||^2+|| $y_i^{[c]}$ ||^2), y_i and $y_i^{[p]}$ are dependent to each other, but the neighbors and cousins are independent to parent. The MAP estimator is used in this model. Maximizing the (7) for each component, we can get

$$y_i = \hat{s}_i - \sigma_n^2 \frac{d \log p_s(s)}{d\hat{s}_i} \quad (8)$$

where, i[I,d]. By the way, the property of the modified Bessel function of the second kind$K_\lambda(u)$ is

$$\frac{d}{du}\log K_\lambda(u) = \frac{\lambda}{u} - \frac{K_{\lambda+1}(u)}{K_\lambda(u)} \quad (9)$$

Then, the second term of Eq.(8) can be computed as

$$\frac{d}{d\hat{s}_i}\log p_s(s) = -\frac{\hat{s}_i}{\|\hat{s}\|}\sqrt{\frac{2}{c}}\frac{K_{d/2-p+1}(\sqrt{2/c}\,\|\hat{s}\|)}{K_{d/2-p}(\sqrt{2/c}\,\|\hat{s}\|)} \quad (10)$$

Though the above eq., the MAP estimator can be formulated using Eq.(7) and Eq.(9), it gives

$$y_i = \hat{s}_i\left[1 + \frac{\sigma_n^2}{\|\hat{s}\|}\sqrt{\frac{2}{c}}\frac{K_{d/2-p+1}\left(\sqrt{2/c}\,\|\hat{s}\|\right)}{K_{d/2-p}\left(\sqrt{2/c}\,\|\hat{s}\|\right)}\right] \quad (11)$$

Then, we approximate the $\|\hat{s}\|$ as $\|y\|$.The multivariate shrinkage function can be written as

$$\hat{s}_i \approx \frac{y_i}{\left[1 + \frac{\sigma_n^2}{\|y\|}\sqrt{\frac{2}{c}}\frac{K_{d/2-p+1}\left(\sqrt{2/c}\,\|y\|\right)}{K_{d/2-p}\left(\sqrt{2/c}\,\|y\|\right)}\right]} \quad (12)$$

where σ_n =*Median*(y_i)*/0.6748*, *p=3/(Kurt(X)-3)*, *c=Var(X)/p*. *X* is the HH subband. Var(*X*) and Kurt(*X*) are the variance and kurtosis.

3. Experimental Results and Discussions

In this section, the examples of image denoising present the proposed models that wasdescribed in the previous section. There are the Windows XP, Core Duo2, 2.0GHz computer for simulations. In the first experiment, this study compares the *Barbara* image denoising, which results with Ref. [3], [7], [8], [9] and [12]. Through Human Visual System (HSV), the study found that the proposed method denoising ability obviously better than the other methods (see Figure 1). The sharpness of the denoised image is close to the original Barbara image. In Figure 2(a) plots the histogram of coefficients of the image Barbara, 512×512 pixels. The kurtosis of the distribution is 20. The Figure 2(b) shows that the coefficients have significantly non-Gaussian statistics, which that are best described by families of heavy-tailed distributions, α= 1.1311.

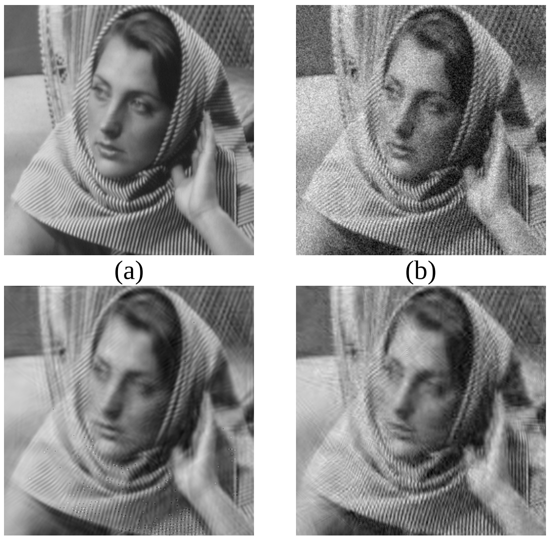

(a) (b) (c) (d)

(e)

(f)

(g)

(h)

Figure 1:Experimental results. (a)Barbara; (b) noisy (σn=20); (c) denoised with K-Sigma1; (d) denoised with K-Sigma2; (e) denoised with BLS-GSM; (f) denoised with GSCE; (g)denoised with Contourlet-HMT; (h) denoised with the proposed NGMS.

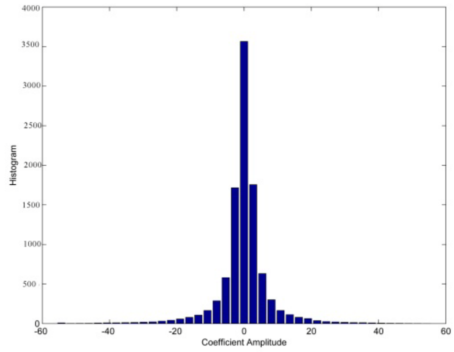

(a)

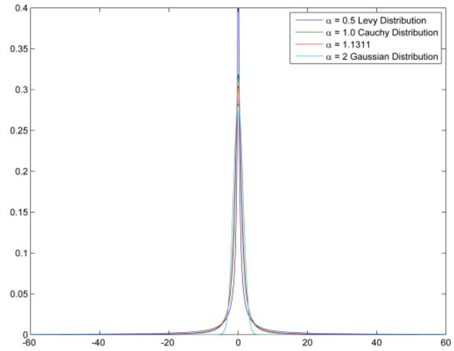

(b)

Figure 2:Marginal statistics of contourlet coefficients of the image "Barbara". (a)Histogram; (b) Statistics distributions of coefficients (α= 1.1311).

Table 1. PSNR values of denoised images for Barbara with different noise levels, K-Sigma1[7], K-Sigma2 [12], BLS-GSM [3], GSCE [8], ContourletHMT [9], and proposed method.

Noise Level	Noisy Image	K-Sigma$_1$	K-Sigma$_2$	BLS-GSM	GSCE	Contourlet-HMT	Proposed
σ_n=10	28.19	28.47	29.28	33.08	31.71	31.40	34.63
σ_n=20	22.13	25.49	26.09	28.93	28.09	26.25	31.40
σ_n=30	18.64	24.56	24.33	26.78	26.07	23.01	28.31

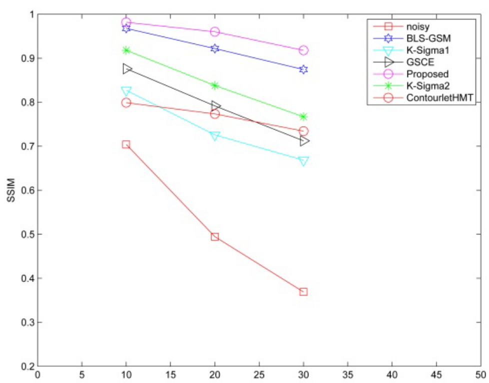

Figure 3: Comparison of denoised results on Barbara in term of SSIM.

From the above table, the study finds that the proposed method is outperformed. The value of SSIM is highest than the others, being the higher is the better. The average improvement in term of PSNR values for test images is approximately 2.5dB. The average CPU processing time of the methods is $CPU_{K\text{-}Sigma1}$=1.94s, $CPU_{BLS\text{-}GSM}$=31.33s, CPU_{GSCE}= 16.11s, $CPU_{K\text{-}Sigma2}$=13.95s, $CPU_{ContourletHMT}$ =18.93 s, and $CPU_{Proposed}$=15.41 s. The processing time of the proposed method is faster than [3], [9], and [8], for example, the Barbara image with abundant texture features. Besides, the study compares Mandrill (512X512 pixels) image with many detail characters. The denoised results are presented on Figure 4, Table 2, 3. The experiment also proved the effectiveness of the proposed algorithm.

Let x_i and y_i be the *i*-th pixel in the original image **x** and the distorted image **y** respectively. The *MSE* and *PSNR* between the two images are given by

$$MSE = \frac{1}{N}\sum_{i=1}^{N}(x_i - y_i)^2, \tag{13}$$

$$PSNR = 10\log_{10}\left(\frac{L^2}{MSE}\right) \tag{14}$$

In Ref. [13,14], a multi-scale SSIM method for image quality assessment is proposed. Input to signal A and B, let μA, σA and σAB respectively as the mean of A, the variance of A, the covariance of A and B. The parameters of relative importance α, β, γ are equal to 1. The SSIM is given as follow:

$$SSIM(\mathrm{x},\mathrm{y}) = \frac{(2\mu_A\mu_B + C_1)(2\sigma_{AB} + C_2)}{(\mu_A^2 + \mu_B^2 + C_1)(\mu_A^2 + \mu_B^2 + C_2)} \tag{15}$$

where C_1, C_2 are small constants.

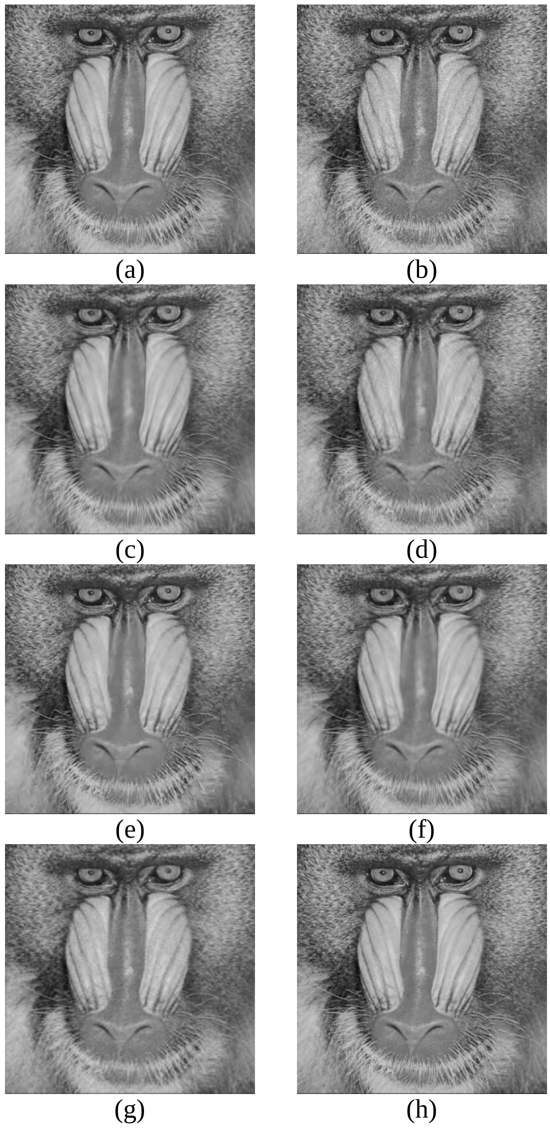

Figure 4:Experimental results. (a)Mandrill; (b) noisy (σn=20); (c) denoised with K-Sigma1; (d) denoised with K-Sigma2; (e) denoised with BLS-GSM; (f) denoised with GSCE; (g)denoised with Contourlet-HMT; (h) denoised with the proposed NGMS.

Table 2.PSNR values of denoised images for Mandrill with different noise levels, K-Sigma1[7], K-Sigma2 [12], BLS-GSM [3], GSCE [8],ContourletHMT [9], and proposed method.

Noise Level	Noisy Image	K-Sigma$_1$	K-Sigma$_2$	BLS-GSM	GSCE	Contourlet-HMT	Proposed
σ_n=10	28.16	24.40	25.72	30.21	26.89	23.97	33.45
σ_n=20	22.14	23.08	22.61	26.11	24.46	23.52	28.21
σ_n=30	18.62	22.22	21.20	24.02	23.05	22.54	25.44

Table 3.SSIM values of denoised images for Mandrill with different noise levels, K-Sigma1[7], K-Sigma2 [12], BLS-GSM [3], GSCE [8],ContourletHMT [9], and proposed method.

Noise Level	Noisy Image	K-Sigma$_1$	K-Sigma$_2$	BLS-GSM	GSCE	Contourlet-HMT	Proposed
σ_n=10	0.8407	0.7125	0.9015	0.9606	0.7879	0.8547	0.9837
σ_n=20	0.6430	0.6267	0.7742	0.8948	0.6943	0.8198	0.8268
σ_n=30	0.4932	0.5548	0.6638	0.8213	0.6103	0.7641	0.7467

As above, table 3 the K-Sigma methods are used the hard-thresholding rule to estimate the unknown wavelet, curvelet or contourlet coefficients, which tends to be unstable. The soft-threshold functions are proposed to improve it, but due to the shrinkage of large coefficients, it tends to have larger bias and decrease the precision of reconstructed signal. BLS-GSM performs a litter bad than the proposed method. The reason is the contourlet transform not only with nearly "completely" decomposition, that is the contourlet coefficients highly reflect the characteristics of the image, but also the coefficient relationships are well considered in the proposed NGMS model. In Ref. [9], the authors considered the coefficient relationships, due to the accuracy of the training HMT model. However, there is also exist some drawbacks. The drawbacks of GSCE are presented in the section 2.

In the third experiment, the study applies the proposed method in processing deep sea acoustic-optical 6 feet tire image in 100 meters depth Ocean. Through the experiment, the distribution of coefficients is also obeying the non-Gaussian distribution. Taking the proposed method for denoising, the value of PSNR is improved nearly 10dB. The Figure 5 displays that after denoising, the curves of the tire are more smoothly than the original one.

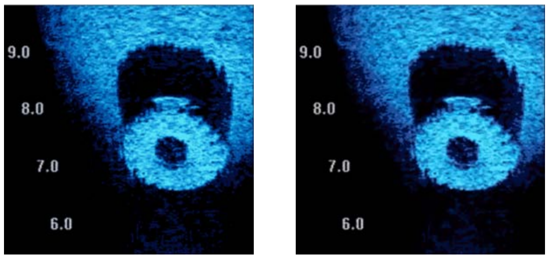

(a) (b)

Figure 5:Deep sea acoustic-optical image denoising results. (a) original image, PSNR=23.87dB; (b) denoised by NGMS, PSNR=33.01dB.

In order to verify the ability and robustness of the proposed method in processing the acoustic-optical underwater images, the study tests 100 groups of images. The average PSNR are shown in Figure 6. From this Figure, it is found that the proposed method is well in donoising acoustic-optical images.

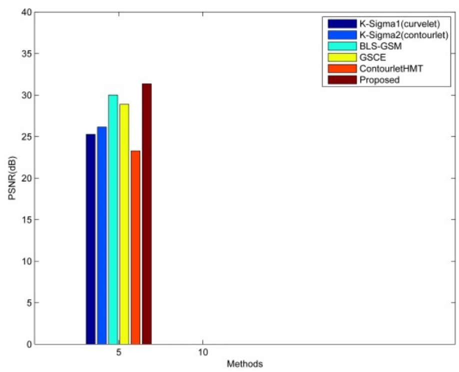

Figure 6:Afterdenoising Average PSNR values of different methods in 100 samples. PSNR(K-Sigma1)=25.28 dB, PSNR(K-Sigma2)=26.16 dB, PSNR(BLS-GSM)=30.01 dB, PSNR(GSCE)=28.89 dB, PSNR(ContourletHMT)=23.28 dB, PSNR(Proposed)=31.36 dB..

4. Conclusions

This paper presents an effective and useful alpha-stable multivariate shrinkage (αMS) model for image denoising, which is based on the MAP estimation and the contourlet transform. We consider the dependencies among a coefficient and parents, and cousins in the αMS model. In order to show the effectiveness of the αMS estimator, three sets of examples are presented and compared with human visual system (HVS) and some well-defined mathematical frameworks. Experimental results demonstrate that the proposed αMS method outperforms the start-of-art methods.

Acknowledgment

This work was partially supported by the Research Found of Japan Society for the Promotion of Science (No.25・10713). The authors gratefully acknowledge the helpful comments and suggestions of the reviewers.

References

[1] E. Belcher, W. Hanot, J. Burch, “Dual-Frequency identification sonar (DIDSON),” Proc. the 2002 International Symposium on Underwater Technology, Tokyo, Japan, pp.187-192, April, 2002.

[2] S.G. Chang, B. Yu, M. Vetterli, “Adaptive wavelet thresholding for image denoising and compression,” IEEE Trans. Image Process., vol.9, no.9, pp.1532-1546, 2000.

[3] L. Sendur, I. W. Selesnick, “Bivariate shrinkage with local variance estimation,” IEEE Sign. Proc. Lett., vol.9, no.12, pp.438-441, 2002.

[4] A. Achim, P. Tsakalides, A. Bezerianos, “SAR image denoising via bayesian wavelet shrinkage based on heavy-tailed modeling,” IEEE Trans. Geos. And Rem. Sens., vol.41, no.8, pp.1773-1784, 2003.

[5] D.L. Donoho, X. M. Huo, “Wedgelets: nearly-minimax estimation of edges,” Annals of Stat., vol.27, no.4, pp.857-897, 1999.

[6] E. Le Pennec, S. Mallat, “Bandelet image approximation and compression,” IEEE Trans. Image Process., vol.14, no.1, pp.423-432, 2005.

[7] J.L. Starck, E. J. Candes, D.L. Donoho, “The curvelet transform for image denoising,” IEEE Trans. Image Process., vol.11, no.6, pp.670-684, 2002.

[8] L. Zhang, Y. Li, H. Lu, S. Serikawa, “Anisotropic multivariate shrinkage function-based image denoising in the second generation curvelet transform domain”, Innovative Computing, Information and Control Express Letters, Part B: Applications, vol.3, no.5, pp.1133-1138, 2012.

[9] D. D-Y. Po, M. N. Do, “Directional multiscale modeling of images using the contourlet transform,” IEEE Trans. Image Process., vol.15, no.6, pp.1610- 1620, 2006.

[10] M.I. Taroudakis, G. Tzagkarakis, P. Tsakalides, “Characterization of an underwater acoustic signal using the statistics of the wavelet subband coefficients,” Jour. of Comp. Acoust., pp.167-174, 2005.

[11] H.M. Lu, L.F. Zhang, S. Serikawa, "Maximum local energy: an effective approach for image fusion in beyond wavelet transform domain," Comp.& Math. with Appl., 2012 (accepted).

[12] M.N. Do, M. Vetterli, "The contourlet transform: an efficient directional multiresolution image representation," IEEE Trans. Image Process., vol.14, no.12, pp.2091-2106, 2005.

[13] Z. Wang, A.C. Bovik, H.R. Sheikh, "Image quality assessment: from error visibility to structural similarity", IEEE Image Proc., vol.13, no.4, pp.600-612, April 2004.

[14] Z. Wang, Q. Li, "Information content weighting for perceptual image quality assessment", IEEE Image Proc., vol.20, no.5, pp.1185-1198, May 2011.

[15] M.I. Taroudakis, G.N. Makrakis, M. Taroudakis, "Inverse problems in underwater acoustics", Springer Press, 2001.

[16] R. Schettini, S. Corchs, "Underwater image processing: state of art of restoration and image enhancement methods", EURASIP J. Adv. Signal Proc., vol.2010, pp.1-14. Feb. 2010.

[17] D.M. Kocak, F.R. Dalgleish, F.M. Caimi, Y.Y. Schechner, "A focus on recent developments and trends in underwater imaging", Marine Tech. Soc. J., vol.42, no.1, pp.52-67, 2008.

Huimin Lu was born in Yangzhou, China. He received the B.S. degree in Electronics Information Science and Technology from Yangzhou University in 2008. And he received M.S. degrees in Electrical Engineering from Kyushu Institute of Technology and Yangzhou University in 2011, respectively. Recently, he is a Ph.D. researcher in Kyushu Institute of Technology. His current research interests include computer vision, communication and deep-sea information processing. He is a member of IEEE, IEICE, ACM and research fellow of JSPS.

Seiichi Serikawa was born in Kumamoto, Japan. He received the B.S. and M.S. degrees in Electronic Engineering from Kumamoto University in 1984 and 1986. From 1990 to 1994, he was an assistant in Kyushu Institute of Technology. He received the Ph.D. degree in Electronic Engineering from Kyushu Institute of Technology, in 1994. From 1994 to 2000, he was an Assistant Professor at the Kyushu Institute of Technology. From 2000 to 2004, he was an Associate Professor at the Kyushu Institute of Technology. Science 2004, he has been a Professor at the Kyushu Institute of Technology. He worked as Vice President of School of Engineering in Kyushu Institute of Technology from 2010 to 2012. Recently, he is the Dean of Department of Electrical Engineering and Electronics of School of

Engineering in Kyushu Institute of Technology. His current research interests include computer vision, sensors, and robotics. He is a member of IEEJ, IEICE, and the president of IIAE.

Lifeng Zhang was born in Dalian, China. He received the B.S. degree in Electronic Engineering from Southeast University in 1994. And he received M.S. and Ph.D. degrees in Electrical Engineering from Kyushu Institute of Technology, in 1999 and 2001, respectively. Recently, he is an assistant Professor in Kyushu Institute of Technology. His current research interests include computer vision, image processing, and communication. He is a member of IIAE, IEEE and IEICE.

Shota Nakashima was born in Fukuoka, Japan. He received the B.S. degree from Nishinippon Institute of Technology in2005. He received the M.S. and Ph.D. degrees in Electrical Engineering from Kyushu Institute of Technology in 2007 and 2010, respectively. From 2010 to 2012, he was an Assistant Professor in Ube National College of Technology. Currently, he is an Assistant Professor in Yamaguchi University. His current research interests include image processing, electronic circuit and artificial life. His current research interests include holography optics, laser design. He is a member of IIAE, and SCIE.